Comparative analyses of three olive mill solid residues from different countries and processes for energy recovery by gasification

Gaëlle Ducom, Mathieu Gautier, Matteo Pietraccini, Jean-Philippe Tagutchou, David Lebouil, Rémy Gourdon

Comparative analyses of three olive mill solid residues from different countries and processes for energy recovery by gasification

G. Ducom, M. Gautier, M. Pietraccini, J.P. Tagutchou, D. Lebouil, R. Gourdon

Comparative analyses of three olive mill solid residues from different countries and processes for energy recovery by gasification

Gaëlle Ducom [a,*], Mathieu Gautier [a], Matteo Pietraccini [a,b], Jean-Philippe Tagutchou[c], David Lebouil [a], Rémy Gourdon [a]

[a] Univ de Lyon, INSA Lyon, DEEP, EA 7429, 20 avenue Albert Einstein, F-69621 Villeurbanne, France

[b] Dipartimento di Scienza Applicata e Tecnologia, Politecnico di Torino, C.so Duca Degli Abruzzi 24, 10129 Torino, Italy

[c] PROVADEMSE, 66 Boulevard Niels Bohr, 69100 Villeurbanne, France

Abstract

Biomass is a renewable energy source which may provide a significant contribution to the reduction of fossil fuels consumption and the associated environmental impacts. The use of agricultural or agro-industrial waste such as solid residues from olive oil production is particularly relevant since it may combine several benefits. Gasification is a promising waste-to-energy technique for this type of lignocellulosic residues. The technology however is adapted to a relatively limited panel of solid waste fuels of defined specifications, which must therefore be characterized properly to assess their adaptation. The purpose of this research was to analyze and compare three different olive mill solid residues by complementary techniques such as Fourier transform infrared spectroscopy (FTIR) and thermochemical methods, in order to characterize these residues as potential fuels for gasification. The results obtained underlined the complex nature of the residues and indicated that they were mainly organic, with very little mineral matter. In addition to the major organic components (cellulose, hemicelluloses and lignin), the presence of several minor organic constituents was shown by thermogravimetry coupled to differential scanning calorimetry and FTIR. The gas produced from pyrolysis was analyzed by gas chromatography and mass spectrometry. It was found to contain several degradation products from lignocellulosic material and olive oil, such as hydroxyacetone, furfural and methoxyphenols. The influence of the olive oil extraction process (two-phase or three-phase) was also demonstrated. It was shown that the thermochemical degradation of olive mill residues followed a complex pathway but the composition of the residues met the requirements for gasification for most parameters.

Keywords: olive mill residues; characterization; thermogravimetry – differential scanning calorimetry; Fourier transform infrared spectroscopy; pyrolysis – gas chromatography/mass spectrometry; gasification

* Corresponding author.

E-mail address: gaelle.ducom@insa-lyon.fr (G. Ducom).

1. Introduction

Mediterranean countries are the largest producers of olive oil in the world. The large quantities of solid and liquid by-products, waste and effluents, generated may significantly affect the economic balance of this agro-industrial activity due to the costs associated to their proper disposal and treatment, or the adverse environmental impacts generated otherwise. In addition, some of these residues may be used as resources for the production of renewable energy, thereby improving furthermore the economic balance.

The nature of solid and liquid residues produced in the olive oil production process depend on the technology used for the extraction of olive oil and the local conditions of operation [1–3]. Three technical options are available for extracting the oil, namely the three-phase and two-phase centrifugation processes, and the traditional pressing process [1;2]. The three-phase process is characterized by the use of large amounts of water to facilitate the extraction and separation of oil, while in the two-phase process, no water is added. Consequently, the three-phase process allows to reach higher oil extraction yields and therefore generates solid organic residues with lower moisture and oil contents, but produces large volumes of aqueous effluents. On the other hand, the two-phase process produces solid residues with higher moisture and oil contents but relatively small volumes of wastewater.

The solid residues generated from olive oil production processes are usually referred to as olive mill solid waste, olive husk or olive pomace. These are mostly lignocellulosic materials made of cellulose, hemicelluloses and lignin, but they also contain residual olive oil, proteins, and various other compounds [1;2]. The type of olives used and their maturity affect the chemical composition of the solid residues, but the extraction process used has a major influence. The solid residues derived from the traditional, two-phase and three-phase processes are significantly different from each other both quantitatively and qualitatively [3]. These differences may suggest different strategies for their treatments, and/or specific adaptations to the treatment processes.

Numerous studies have been published on the possible treatments of olive mill solid waste. Treatments include composting, extraction of valuable products, livestock feeding, land application or the production of derived materials which can be used as soil conditioners or biosorbents for the removal of heavy metals or dyes from industrial effluents [2;4]. More recently, treatment processes for energy recovery have gained increasing interest [3;5]. Indeed, biomass is a renewable energy source which significantly contributes to the reduction of fossil fuels consumption and the associated environmental impacts. Biomass to energy systems are considered environmentally- and climate-friendly options due to their close to neutral balance in greenhouse gas emissions. Using biomass residues is an even better option because it avoids the potential impacts of dedicated energy crops production. Waste-to-energy techniques include biochemical and/or thermochemical conversion technologies. Anaerobic digestion of olive pomace has been extensively studied [6–12]. Thermochemical conversion technologies include pyrolysis, gasification and combustion [13–25].

Gasification is a mature technology for coal or wood conversion and an attractive alternative to combustion for organic residues from agriculture and agro-industry. This thermochemical process converts solid lignocellulosic materials into a gaseous fuel called syngas, mainly composed of hydrogen, carbon monoxide and carbon dioxide. Water, light hydrocarbons such as methane, and nitrogen may also be present among many other trace components. The overall process of gasification is generally considered to comprise four steps occurring in different zones within the gasifier (namely drying, pyrolysis, oxidation and reduction) and involving several simultaneous chemical reactions. The technology however is adapted to a relatively limited panel of solid waste fuels of defined specifications, which must therefore be characterized properly to assess their

adaptation.
Classical waste fuel analyses include proximate analyses (moisture, volatile matter, fixed carbon, and ash contents), ultimate analyses (C, H, N, O and other elements contents), heating value and physical parameters such as bulk density or particle size distribution. Other analytical techniques may provide however more specific information on the considered waste material with respect to its treatability by thermochemical processes such as gasification.

The purpose of this research was to characterize and compare three solid residues collected from olive oil production facilities located in three different Mediterranean countries using different oil-extraction processes. Complementary analytical methods were used such as Fourier transform infrared spectroscopy (FTIR), simultaneous thermogravimetry and differential scanning calorimetry (TG-DSC) and analytical pyrolysis combined with gas chromatography and mass spectrometry (Py–GC/MS). The influence of the oil extraction process on the characteristics of the residues was considered more particularly because the residual oil content is known to affect the gasification process, syngas composition, and the efficiency of pelletizing or briquetting operations which are usually needed to prepare the waste materials for gasification.

2. Material and methods

2.1 Solid residues

Three olive mill solid residues of different origins were compared in the present study. The samples were respectively collected from:
- a three-phase industrial olive oil extraction plant located in Tunisia (referenced 3P-I-T for "3-phase, industrial, Tunisia" in this paper). A representative sample was taken from the production facility by a Tunisian partner (ENIT). The initial moisture content was 52% w/w. The sample was dried in a stove at 50 °C for 24 h prior to being sent to Lyon.
- a three-phase artisanal plant located in the south of France (sample 3P-A-F for "3-phase, artisanal, France"). The initial moisture content was 63% w/w.
- a two-phase industrial plant located in Spain, named 2P-I-S ("2-phase, industrial, Spain"). The solid residues were dried on the facility, further extracted with hexane to recover residual oil contents, and then pelletized. The sample was sent to Lyon in the form of pellets. Initial moisture content was not recorded. However, it is known to range typically around 55-70% w/w [3].
All samples were finely grinded using an agate mortar before analysis.

2.2 Routine analyses

2.2.1 Proximate analyses and higher heating value

Volatile Matter (VM) content was determined as the percentage of mass loss recorded by thermal treatment of dried samples in a closed crucible at a temperature of 900 °C for 7 min in a reductive atmosphere.
Ash content was determined as the mass fraction remaining after complete combustion in air at 600 °C of dried samples.
Fixed carbon (FC) was calculated by mass balance as: FC (%) = 100% − VM (%) – Ash (%).
The higher heating value (HHV) was determined by combustion using a bomb calorimeter.

The lower heating value (LHV) was calculated by subtracting the latent heat of vaporization of water from the HHV:

$LHV\ (MJ/kg_{DM}) = HHV\ (MJ/kg_{DM}) - 2.45 \times 9 \times H$

where 2.45 is the heat of vaporization of water at 20 °C expressed in MJ/kg, 9 is the molar mass ratio between H_2O and H_2 and H is the hydrogen content expressed in % w/w of DM as determined in the elemental analysis (§ 2.2.2).

All analyses were done in triplicates.

2.2.2 Ultimate analysis and metal contents

Total elemental contents (C, H, N, Cl and S) were determined by combustion of dried samples in a bomb calorimeter, followed by the analysis of CO_2, H_2O, N_2, NOx, HCl and SOx. The O content was obtained by difference.

Metal contents (Ag, Al, As, B, Ba, Be, Bi, Ca, Cd, Co, Cr, Cu, Fe, Hg, K, Li, Mg, Mn, Mo, Na, Ni, P, Pb, Sb, Se, Si, Sn, Sr, Ti, Tl, V, W, Zn, Zr) and S content were determined by mineralization and extraction with aqua regia, then metal analysis by inductively coupled plasma mass spectrometry (ICP-MS).

2.2.3 Fiber analyses

Fiber contents were determined following the standard procedure XP U44-162 [26] developed from Van Soest's sequential extraction method [27]. The method consisted in three successive stages of extraction with reagents of increasing hydrolytic strength. After a preliminary extraction with acetone to remove residual oils, the samples were extracted with a neutral detergent aqueous solution to collect the easily extractible constituents. The residual solids were dried and weighed. They constituted the neutral detergent fiber (NDF) fraction. The solids in NDF fractions were predominantly composed of cellulose, hemicelluloses and lignin. NDF fraction was then treated with a dilute acidic detergent aqueous solution. This stage hydrolyzed hemicelluloses which were hence separated as soluble products of hydrolysis from the solid fraction called ADF (for acid detergent fraction). The ADF solids were further treated with a concentrated sulfuric acid aqueous solution to hydrolyze cellulose. The remaining solids constituted ADL fraction and were considered to contain mostly lignin. They were weighed, dried at 105 °C, weighed again and calcined at 480 °C for 6 h in a furnace.

The procedure allowed to determine the contents in "extractives" (easily soluble constituents), hemicelluloses, cellulose and lignin, expressed in % w/w of dry matter, as follows:

- Extractives = (total initial dry mass – dry mass of NDF fraction) / total initial dry mass;
- Hemicelluloses = (NDF – ADF) / total initial dry mass;
- Cellulose = (ADF – ADL) / total initial dry mass;
- Lignin = ADL / total initial dry mass.

2.3. Fourier transform infrared spectroscopy (FTIR)

The three samples were analyzed by Fourier transform infrared spectroscopy in attenuated total reflectance (ATR) mode with a Nicolet IS50 equipment. FTIR analyses allow the characterization of the nature of inter-atomic bonds present in the constituents of the material from their typical vibration frequency (stretching and bending). FTIR spectra were recorded between 500 and 4000 cm^{-1} with a resolution of 4 cm^{-1}. OMNIC software was used for data acquisition and post-treatment.

2.4. Thermogravimetry (TG) and differential scanning calorimetry (DSC)

Thermogravimetry and differential scanning calorimetry were performed on the three samples both in nitrogen and in air, using a Mettler Toledo TGA/DSC 2 thermal analyzer. The device was equipped with a thermobalance, and recorded as a function of temperature both the sample's mass evolution (TG) and the heat flow variation between the sample and a reference material (DSC). Samples of approximately 20 mg were introduced into an alumina crucible and heated from 25 °C to 950 °C according to the following pattern: heating from 25 to 105 °C at a rate of 10 °C/min, plateau at 105 °C for 15 minutes (to remove all the water), then heating from 105 to 950 °C at a rate of 5 °C/min.

2.5. Analytical pyrolysis combined with gas chromatography/mass spectrometry (Py–GC/MS)

Dried samples of 1-2 mg were flash-pyrolyzed at 550 °C in inert atmosphere (helium) using an EGA/PY-3030D Pyrolyzer. The gas emitted was analyzed with a gas chromatograph (GC7890A from Agilent) and a mass spectrometer (5977B from Agilent). The GC oven program temperature was: 50 °C for 5 minutes, heating rate of 15 °C/min (50 to 280 °C), 280 °C for 5 minutes. The method allowed to identify the main families of constituents in the pyrolysis gas and analyze them semi-quantitatively. Each sample was analyzed in triplicate.

3. Results

3.1 Routine analyses

The results of proximate and ultimate analyses, metal contents, HHV determination and fiber analysis are given in Table 1. Standard deviations are given when triplicate analyses were done. Note that the metals analyzed at a content below 10 mg/kg_{DM} or below their respective limits of quantification were not included in Table 1.

Table 1

Chemical composition of olive mill solid residues: proximate analysis, ultimate analysis, metal contents, higher heating value and fiber analysis (DM: dry matter).

Parameter	3P-I-T	3P-A-F	2P-I-S
Volatile matter (% w/w of DM)	80.0 ± 1.5	79.0 ± 0.4	73.5 ± 0.2
Fixed carbon (% w/w of DM)	17.6 ± 1.5	17.9 ± 0.3	17.6 ± 0.2
Ash (% w/w of DM)	2.5 ± 0.2	3.1 ± 0.2	8.9 ± 0.1
C (% w/w of DM)	55.1	53.3	48.4
H (% w/w of DM)	7.0	7.2	6.0
O (% w/w of DM)	33.9	35.2	34.9
N (% w/w of DM)	1.3	1.0	1.5
K (mg/kg_{DM})	11300	12400	19700
Ca (mg/kg_{DM})	14800	2200	7250
P (mg/kg_{DM})	1080	1490	1650
Cl (mg/kg_{DM})	1400	850	2000
S (mg/kg_{DM})	1280	797	1250
Mg (mg/kg_{DM})	667	489	1180
Fe (mg/kg_{DM})	258	143	484
Na (mg/kg_{DM})	557	46	103
Si (mg/kg_{DM})	197	28	270

Al (mg/kg$_{DM}$)	142	23	323
Zn (mg/kg$_{DM}$)	15	351	24
B (mg/kg$_{DM}$)	26.2	16.2	39.9
Cu (mg/kg$_{DM}$)	10.9	16.1	16.5
Mn (mg/kg$_{DM}$)	16.9	8.7	20.6
Sr (mg/kg$_{DM}$)	63.1	< 5.0	52.3
Zr (mg/kg$_{DM}$)	2.2	6.0	22.9
HHV (MJ/kg$_{DM}$)	22.0 ± 0.3	22.7 ± 0.3	19.7 ± 0.1
LHV (MJ/kg$_{DM}$)	20.4 ± 0.3	21.1 ± 0.3	18.3 ± 0.1
Extractives (% w/w of DM)	34.0 ± 1.3	46.0 ± 0.4	47.3 ± 0.9
Cellulose (% w/w of DM)	33.8 ± 0.5	27.7 ± 0.6	24.8 ± 1.6
Hemicelluloses (% w/w of DM)	16.3 ± 2.3	13.0 ± 0.4	14.5 ± 1.5
Lignin (% w/w of DM)	15.8 ± 0.7	13.3 ± 0.5	13.4 ± 0.5

Analytical data gathered in Table 1 revealed quite similar compositions of the three samples. Analyzed compositions were also close to literature data reported for olive mill residues of other origins [1;17;28−30].

Regarding proximate and ultimate analyses, no significant difference was observed between the 3P-I-T and the 3P-A-F samples. Yet, some differences were observed mostly between sample 2P-I-S and the others: lower VM content, lower C and H contents, and higher ash content. These differences were attributed to the stage of hexane extraction on 2P-I-S sample which, by removing residual oil, decreased volatile matter content of the residues. The lower contents in C and H of 2P-I-S sample were also good indicators of its lower residual oil content since fatty acids in the oil are mostly composed of C and H. Finally, these observations were consistent with the lower heating value of sample 2P-I-S as compared to the other two samples. Fixed carbon content was similar in the three samples.

The metals found in highest concentrations were K, Ca and P, followed by Mg, Fe, Na, Si, Al and Zn. The highest content in K was observed in the 2P-I-S sample and the highest content in Ca was observed in the 3P-I-T sample. The contents in several toxic metals or metalloids such as As, Cd, Cr, Hg, Pb, Sb and Se were below the limits of quantification. The lowest Cl and S contents were observed in the 3P-A-F sample. The observed differences in metals, Cl and S contents may be correlated to olive type and growing conditions.

With regards to fiber analysis, the three samples revealed high contents in extractives, although sample 3P-I-T was at a significantly lower level than the other two samples. Extractives are composed of a variety of constituents relatively easily extractible by a neutral detergent, such as oils (glycerol tri-esters), waxes, terpenes, fatty acids, alcohols, alkanes, gums, phenolic compounds, carbohydrates, etc. The content in cellulose was significantly higher in the 3P-I-T sample and significantly lower in the 2P-I-S sample. The content in hemicelluloses was similar in the three samples whereas lignin content appeared slightly higher in the 3P-I-T sample. The observed differences in fiber contents may be explained by factors such as the type of olives or their growing conditions or their maturity.

3.2 Fourier transform infrared spectroscopy

Figure 1 shows the FTIR spectra obtained for the 3 samples. Even if strong similarities could be observed between the 3 samples from these analyses, some differences were also highlighted.

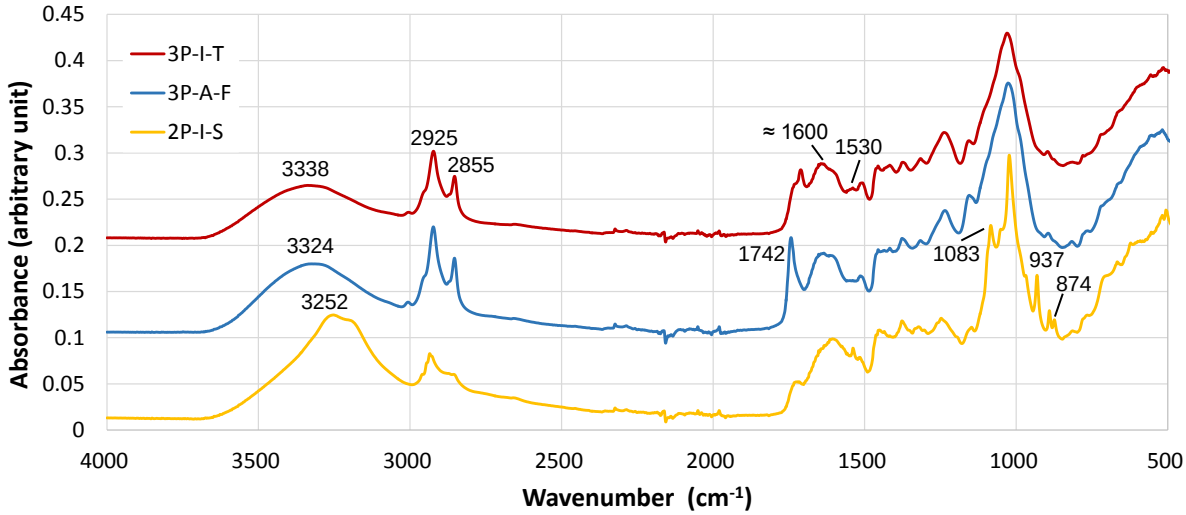

Figure 1. FTIR spectra recorded from the samples 3P-I-T, 3P-A-F and 2P-I-S.

A broad band in the range 3100-3700 cm^{-1} was recorded for the three samples, corresponding to the OH stretching region. It can be assigned to OH vibrations in carboxylic groups, alcohols or phenols. Several compounds, such as cellulose, hemicelluloses and lignin may explain the presence of these vibrations. It was observed that this peak was shifted to lower wavenumbers in 2P-I-S sample (maximum at 3252 cm^{-1}) as compared to 3P-I-T and 3P-A-F samples (3338 and 3324 cm^{-1} respectively), revealing a different structure of the molecule bearing the –OH group.

The very weak peak observed in 3P-I-T and 3P-A-F samples around 3000 cm^{-1} was assigned to C-H stretching vibration in RHC=CHR. The two sharp peaks around 2925 and 2855 cm^{-1} were due to vibrations of asymmetric and symmetric -C-H stretching band in aliphatic chains [31]. They were observed in all samples, although slightly smaller in 2P-I-S sample.
In the 1200-2000 cm^{-1} range, several peaks specifically attributed to organic compounds were observed, underlining the complex structure of the samples. The bands in the range of 1742-1710 cm^{-1} can be assigned to C=O stretching in carbonyl of esters and in carboxylic groups. Some differences were observed between the three samples in terms of wavenumber (from 1710 to 1742 cm^{-1}) and intensity for these characteristic bands. The broad bands around 1600 cm^{-1} could be attributed to C=C stretching in alkenes and aromatic compounds, with contributions of C=O stretching of ketones [32]. The band around 1530 cm^{-1} showed C-N stretching vibrations in combination with N-H bending (called the Amide II band).
The region between 1200 and 1400 cm^{-1} was assigned to methyl symmetrical bending, -COO- symmetrical stretching vibration and C-O stretching in carboxylic acids [33;34]. The bands between 850 and 1200 cm^{-1} may be attributed mainly to O-H stretching in organic compounds, but also in some mineral phases, and to C-O stretching in carboxylic groups of organic molecules [35;36].
The spectra recorded from samples 3P-I-T and 3P-A-F were very similar to each other. The spectrum recorded from 2P-I-S sample showed however significant differences, such as sharp specific bands at 1083, 937 and 874 cm^{-1} which were not observed in 3P-I-T and 3P-A-F samples. FTIR therefore confirmed the routine analyses, showing very close similarities between 3P-I-T and 3P-A-F samples, which were both produced from a three-phase extraction process, while revealing a slightly different profile for 2P-I-S sample, originating from a two-phase process followed by hexane extraction of residual oil.

3.3. Thermogravimetry and differential scanning calorimetry

TG-DSC analyses were performed in both oxidative (air) and inert (N_2) atmospheres in order to investigate the processes occurring respectively in the pyrolysis and oxidation zones of the gasifier. Only the phenomena occurring above 105 °C were considered here (i.e after the total removal of water in the thermal analyzer).

3.3.1. TG-DSC in air

Figure 2 shows the TG (mass loss) and DSC (heat flux) profiles obtained for the three olive mill residues in oxidative atmosphere (air). Derivative thermogravimetric curves (dTG) are also shown.

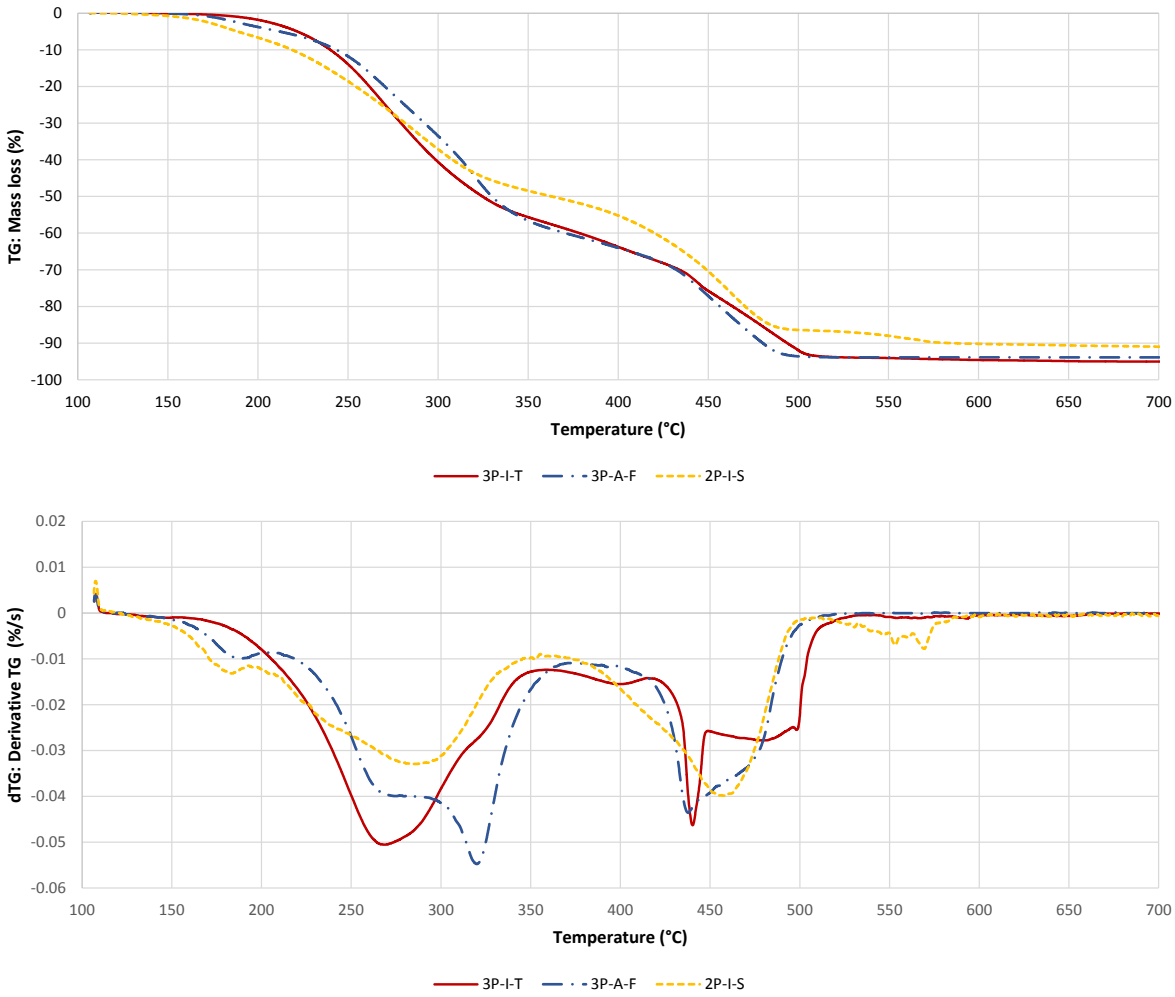

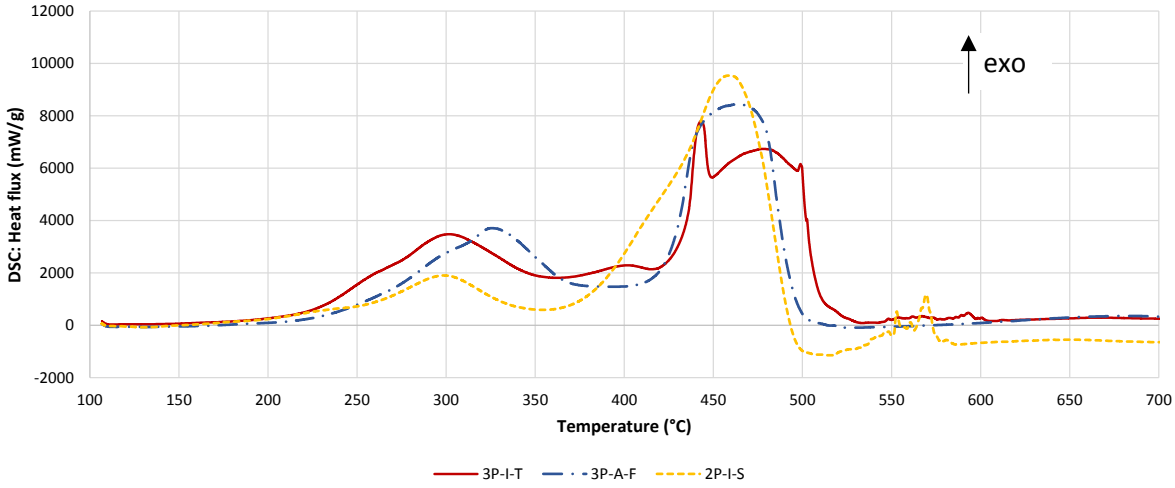

Figure 2. TG, dTG and DSC profiles for the three samples (3P-I-T, 3P-A-F, 2P-I-S) under air atmosphere (heating rate 5 °C/min).

The baseline considered as mass reference for the calculation of mass loss and heat flux was the sample mass after the plateau at 105 °C (i.e. after complete drying).
For the three samples, the TG curves showed two main regions for mass losses associated in DSC with exothermic peaks (centered at 290-320 °C and 440-480 °C). Several authors described the oxidative thermal degradation of olive pomace or other biomass as a progressive decomposition of cellulose, hemicelluloses and lignin into volatiles and solid char, followed by the combustion of solid char generated by pyrolysis [22;24;37].
The cumulated mass loss recorded over the whole range of temperatures of the assays was around 94-95% w/w of dry matter for 3P-I-T and 3P-A-F samples, and 91% for 2P-I-S sample. This mass loss mainly occurred below 550 °C, indicating that the residues were mainly organic, with small contents in inorganic matter. These results are in accordance with the ash contents given in Table 1.
The mass loss related to the first peak in TG curves was around 45 % w/w of initial dry mass with 2P-I-S sample and around 60% for 3P-I-T and 3P-A-F samples. Another noticeable difference was that exothermic reactions were of smaller amplitude for the first peak and higher amplitude for the second peak in 2P-I-S sample. These observations were attributed to hexane extraction in the two-phase process, which removed residual oil and also probably part of the relatively easily degradable organic matter.
Slighter differences were also observed between 3P-I-T and 3P-A-F samples, with respect to the dTG and DSC curves maxima. They underlined the complex nature of the residues, composed of several groups of organic constituents, which are oxidized at different temperatures, even for residues generated from the same process of oil extraction.
DSC and dTG curves were further analyzed by deconvolution. As an example, figure 3 shows the deconvolution result of the DSC curve for the sample 3P-I-T. For a good fit between the experimental and deconvoluted dTG and DSC curves of samples 3P-I-T and 3P-A-F, a deconvolution into at least 9 overlapping peaks was necessary. As for sample 2P-I-S, a good fit was obtained with 7 peaks of deconvolution. The higher number of peaks for 3P-I-T and 3P-A-F as compared to 2P-I-S sample may be attributed to the reactions of the residual oils remaining in 3P-I-T and 3P-A-F samples. Vecchio et al. [38] studied the thermal decomposition of 12 monovarietal extra virgin olive oils in air and observed a complex multistep decomposition pattern with several overlapping processes due to the

chemical composition of the samples, including triacylglycerols, fatty acids and phenols. In their study, all DSC thermograms were best deconvoluted into six Gaussian peaks.
Moreover, a two-stage char combustion process has also been reported for some biomass samples [30].

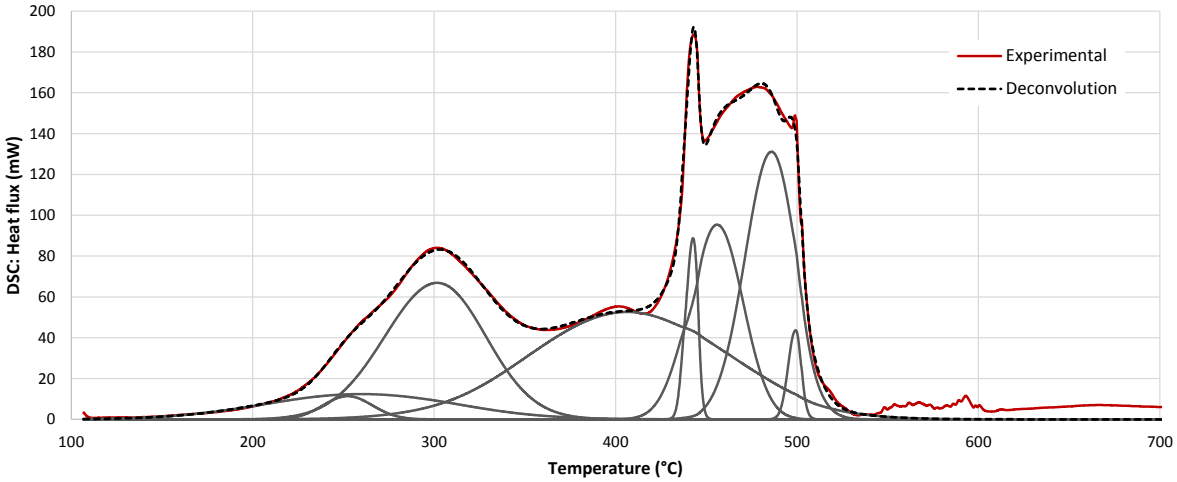

Figure 3: Deconvolution of the DSC curve for the 3P-I-T sample.

3.3.2. TG-DSC in nitrogen

Figure 4 shows the TG, dTG and DSC profiles obtained for the three olive mill residues (3P-I-T, 3P-A-F and 2P-I-S) in inert atmosphere (nitrogen).

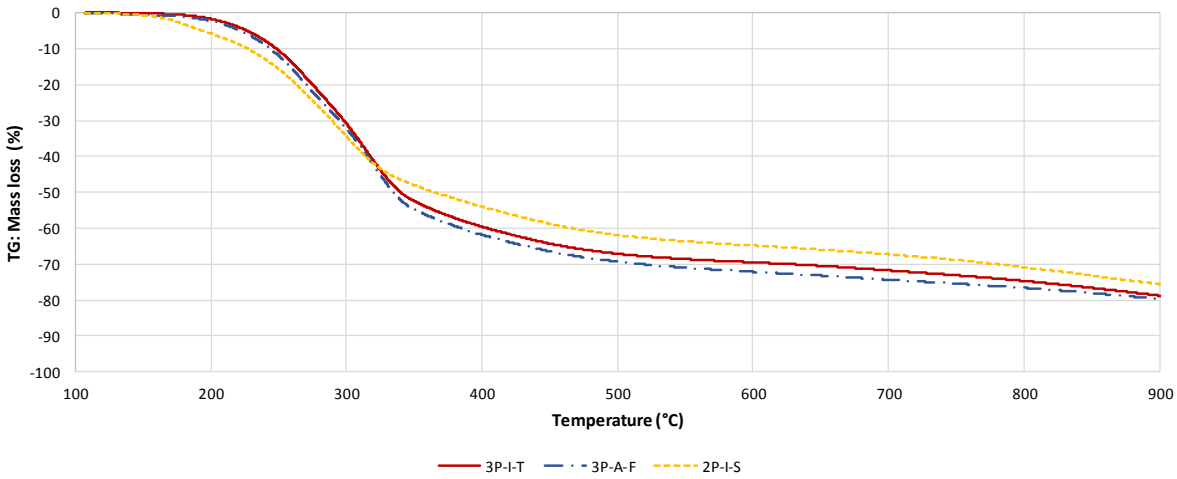

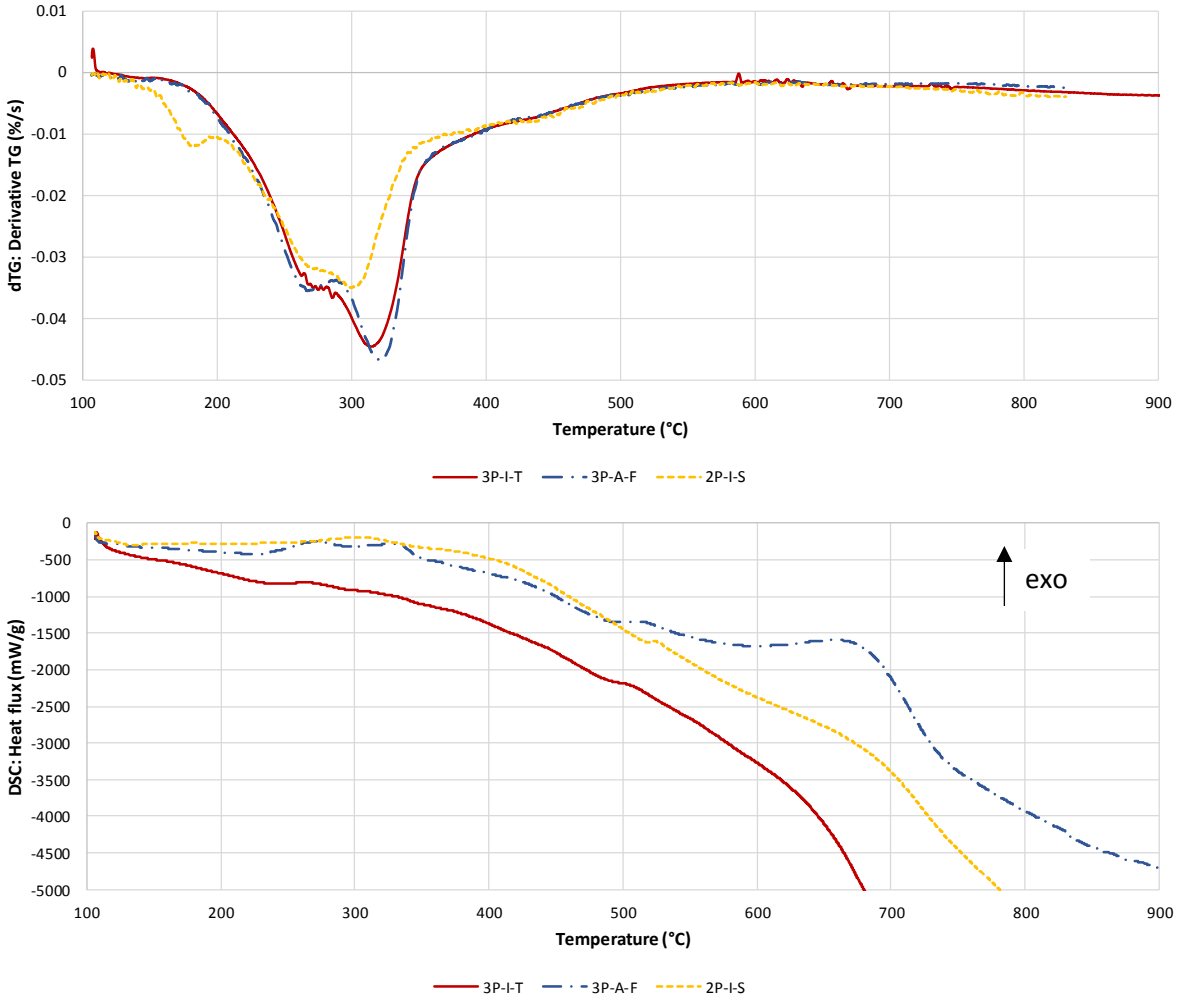

Figure 4. TG, dTG and DSC profiles for the three samples (3P-I-T, 3P-A-F, 2P-I-S) under N_2 atmosphere (heating rate 5 °C/min).

The TG curves obtained in N_2, assimilated to pyrolysis profiles, showed two main mass loss contributions in the 200-600°C region with associated endothermic reactions of low intensities in DSC. A similar trend was reported for olive mill residues by Darvell et al. [30] and Gomez-Martin et al. [24]. The first peak around 250 °C, also considered as a shoulder of the main peak (dTG curve), is commonly attributed to the decomposition of hemicelluloses. The main peak at higher temperature (maximum between 300 and 325 °C here) was attributed to cellulose decomposition. Lignin decomposition occurred over a large temperature range, explaining the slow mass loss observed at temperatures upper 350 °C [39;40].

The overall mass losses measured in N_2 were around 84%, 83% and 80% w/w of dry matter for samples 3P-I-T, 3P-A-F and 2P-I-S respectively. They were lower than in air, which was attributed to the presence of a residual mass of char, which remained at the end of thermal analyses in nitrogen, whereas char was fully oxidized in air. Finally, the TG profile of sample 2P-I-S differed from those of the other two samples with a smaller mass loss in the lower temperature mass-loss zone.

A good fit of the experimental dTG curves was obtained with a deconvolution in 5 peaks for the three samples. The lower number of peaks compared to the results in air atmosphere is partly due to the fact that there is no char combustion in nitrogen.

3.4 Analytical pyrolysis combined with gas chromatography/mass spectrometry

The three samples were analyzed by pyrolysis combined with gas chromatography and mass spectrometry. Figure 5 shows the raw spectra obtained with the three samples. The y-axis is abundance and the x-axis is the retention time (depending on the GC program).

From 3 to 17 min, numerous peaks were recorded, which were mainly attributed to substituted phenols. The peaks observed at higher retention times (> 17 min) were attributed to tyrosol and fatty acids (retention time of 17-21 min) and squalene (retention time of 24 min).

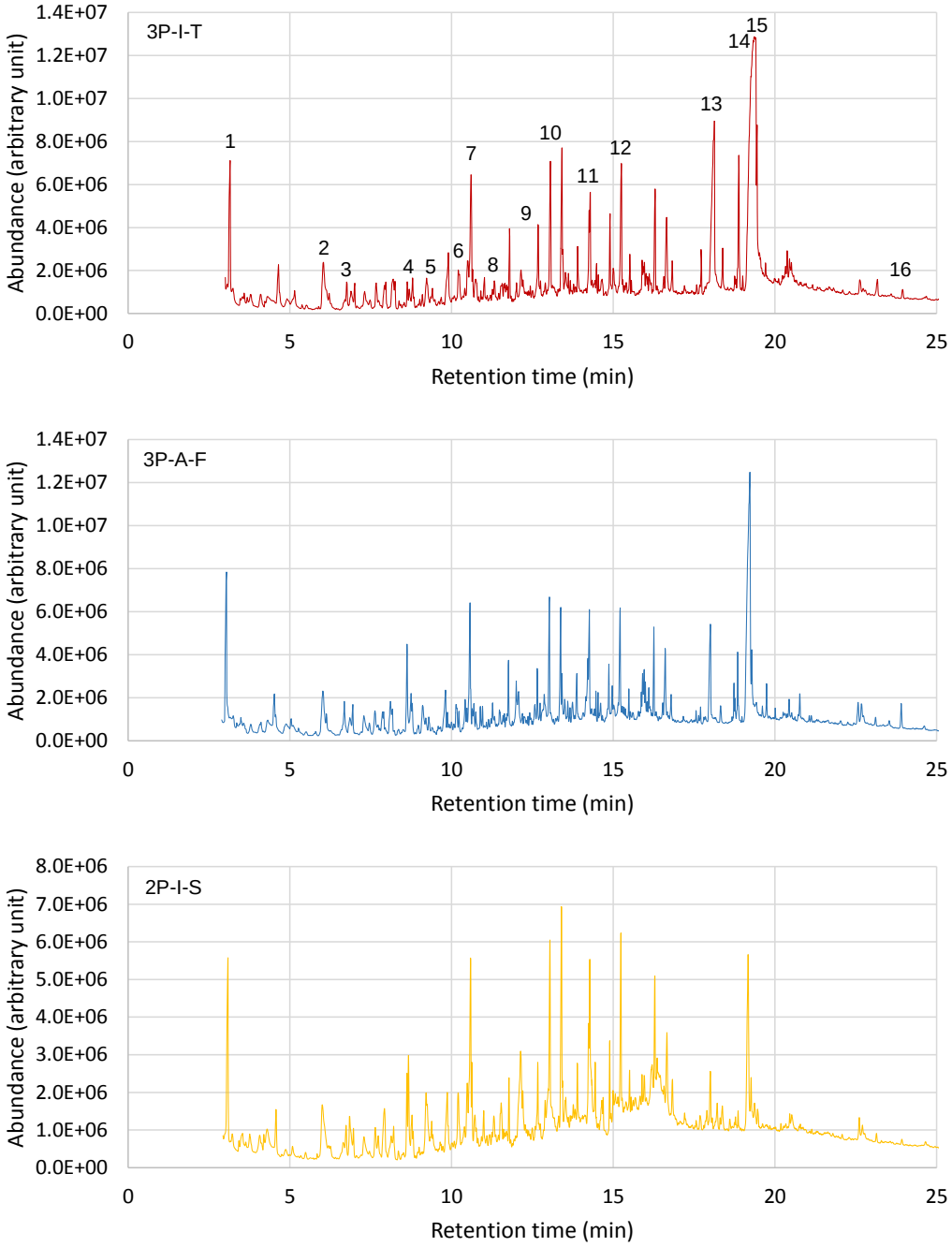

Figure 5: Py–GC/MS chromatograms of the three samples (3P-I-T, 3P-A-F, 2P-I-S).

Nineteen compounds of interest were clearly identified from the collected chromatograms. These compounds were of two types of origins. A first group of compounds (mostly phenols and substituted phenols) were produced from the thermal degradation of the lignocellulosic structural material of the samples (Figure 6). A second group of compounds were formed by the vaporization or (partial) degradation of the residual olive oil constituents (Figure 7). Assignments of the main peaks are presented in Table 2 where m/z is the mass-to-charge ratio. Benzene, toluene and naphthalene were also found in the pyrolysis gas but were not included because their contents were very low.

Table 2
Assignments of the main peaks identified in the Py–GC/MS chromatograms

Peak	Compound	Formulae	m/z	Marker
1	Hydroxyacetone	$C_3H_6O_2$	43	cellulose and hemicelluloses
2	Furfural	$C_5H_4O_2$	96	cellulose and hemicelluloses
3	2-Furanemethanol	$C_5H_6O_2$	98	cellulose and hemicelluloses
4	Ethylpyridine	C_7H_9N	107	amino acids and proteins
5	Phenol	C_6H_6O	94	p-hydroxyphenyl lignin
6	Cresol	C_7H_8O	107	p-hydroxyphenyl lignin
7	2-Methoxyphenol	$C_7H_8O_2$	109	guaiacyl lignin
8	4-Ethylphenol	$C_8H_{10}O$	107	p-hydroxyphenyl lignin
9	2-Methoxy-4-vinylphenol	$C_9H_{10}O_2$	150	p-hydroxyphenyl lignin
10	2,6-Dimethoxyphenol	$C_8H_{10}O_3$	154	syringyl lignin
11	Tyrosol	$C_8H_{10}O_2$	107	Oil
12	2,6-Dimethoxy-4-ethylphenol	$C_{10}H_{14}O_3$	180	syringyl lignin
13	Palmitic acid	$C_{16}H_{32}O_2$	73	Oil
14	Oleic acid	$C_{18}H_{34}O_2$	55	Oil
15	Stearic acid	$C_{18}H_{36}O_2$	73	Oil
16	Squalene	$C_{30}H_{50}$	69	Oil

The degradation products are shown on Figure 6 and Figure 7, which compare the abundance of the major compounds identified in the gases collected from the pyrolysis of the three samples. The y-axis shows the surface areas of the peaks corresponding to the different compounds obtained from the pyrolysis of 1 mg of each dried sample.
Several authors reported that hydroxyacetone, furfural and 2-furanemethanol come from the thermal degradation (pyrolysis) of cellulose and hemicelluloses [30;41−44].
Lignin is a complex three-dimensional amorphous macromolecule made from the polymerization of three phenylpropane units: p-hydroxyphenyl, guaiacyl and syringyl in proportions which depend on the origin of the molecule. Some published studies [30;41;42] have demonstrated that:
- phenol, cresol, 4-ethylphenol and 2-methoxy-4-vinylphenol are produced from the pyrolysis of p-hydroxyphenyl lignin;
- 2-methoxyphenol is a product from the pyrolysis of guaiacyl lignin;
- 2,6-dimethoxyphenol and 2,6-dimethoxy-4-ethylphenol come from the pyrolysis of syringyl lignin.

Ethylpyridine was also identified in the pyrolysis products (Figure 6). It is produced from the degradation of amino acids and proteins [45] and therefore can be used as an indicator of the presence of organic nitrogen in the analyzed sample.

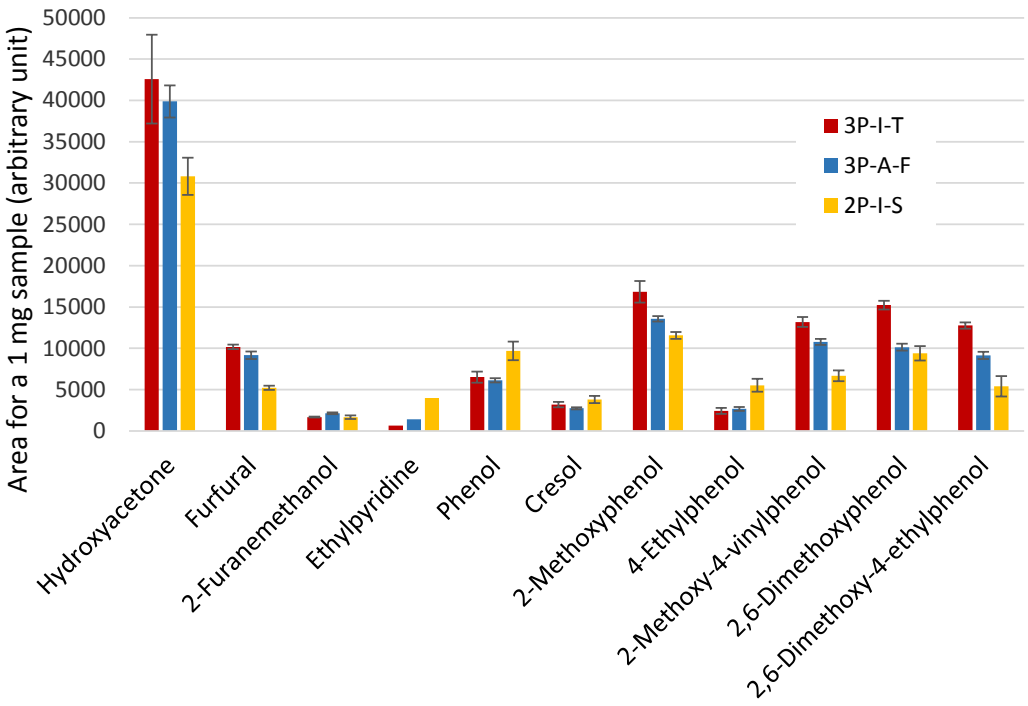

Figure 6: Contents in degradation products from the lignocellulosic material and proteins in the pyrolysis gas from the three samples (3P-I-T, 3P-A-F, 2P-I-S).

Figure 6 shows that the three samples revealed relatively similar profiles. Some differences were observed however on sample 2P-I-S, which produced the smallest quantities of most identified compounds (hydroxyacetone, furfural, methoxyphenols, etc.) while revealing the highest concentrations in a few other constituents (phenol, ethylpyridine, 4-ethylphenol).
Sample 3P-I-T also revealed slight differences as compared to the others, with the highest contents in methoxy- and dimethoxy-phenols, which are produced from thermal degradation of lignin. It may be explained by the fact that the lignin content was slightly higher in the 3P-I-T sample, as shown in Table 1.

The second group of products identified in the pyrolysis gas were produced by the vaporization and/or (partial) degradation of residual olive oil, namely tyrosol, palmitic acid, oleic acid, stearic acid and squalene (Figure 7). These compounds have been reported as typical constituents of olive oil [46–48].
The highest contents in palmitic acid, oleic acid and stearic acid were obtained in the pyrolysis gas from sample 3P-I-T, which was thereby identified as the residue with the highest residual oil content. The pyrolysis gas from 2P-I-S showed on the contrary the lowest abundance in these compounds and in squalene. This result was consistent with the very low residual oil content in sample 2P-I-S due to hexane extraction.
The high content of tyrosol found in the 2P-I-S sample could be surprising. Tyrosol is a phenolic compound classically found in olive oil where it forms esters with fatty acids. The lower quantity of acids in 2P-I-S could explain this presence because tyrosol content seems to be anticorrelated to acid content.

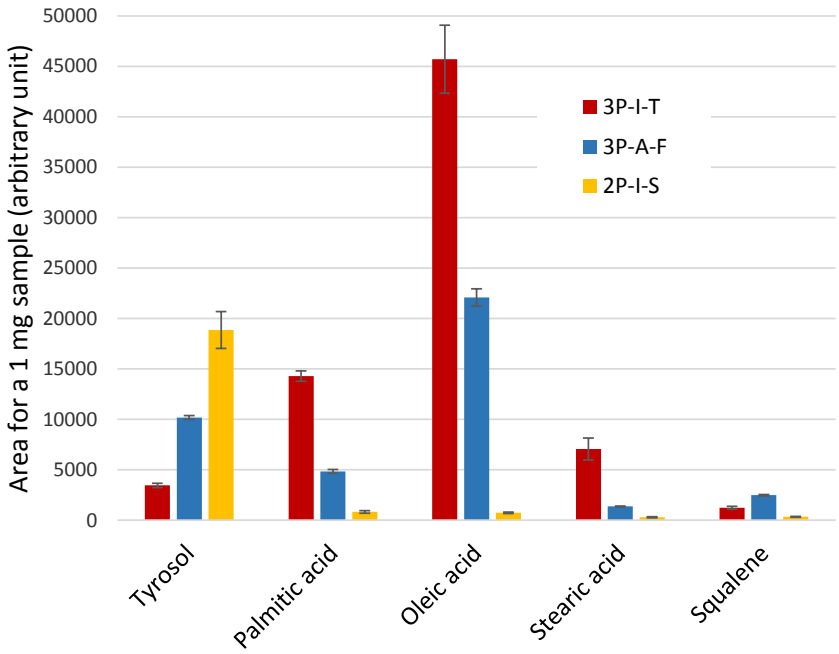

Figure 7: Tyrosol, palmitic acid, oleic acid, stearic acid and squalene contents in the pyrolysis gas from the three samples (3P-I-T, 3P-A-F, 2P-I-S).

4. Discussion

4.1 Suitability of olive mill solid residues for gasification

The International Energy Agency (IEA) recently published a detailed report on the pretreatment of biomass residues in the supply chain for thermal conversion [49]. The report considers both refuse derived fuels (RDF), which are primarily targeted for combustion, and solid recovered fuels (SRF), which are more strictly defined sorted waste. A standard for SRF is under development (ISO/TC300). The report provides the following requirements and specifications for fuels feeding a circulating fluidized bed gasifier:

- moisture content ≤ 35% w/w;
- LHV in the order of 10-20 MJ/kg ;
- ash content ≤ 25% w/w;
- sulfur ≤ 1% w/w, chlorine ≤ 2% w/w, mercury ≤ 1.5 mg/kg;
- ash melting point ≥ 960 °C.

It also reports that SRFs with a VM content in the range of 76−86% were already successfully used in gasification in several case studies.

The typical humidity of solid olive mill waste is usually higher than recommended, ranging between 40−45% w/w for three-phase processes and 55−70% w/w for two-phase olive mill waste [3]. A drying step would therefore be necessary. In most Mediterranean countries, sun drying can be a low-cost effective option. Humidity is particularly crucial in the pretreatments of aggregation which are needed before gasification. Al-Widyan and Al-Jalil [50] showed that the durability of olive cake briquettes increased from about 10 to 100% with increasing initial moisture content from 20 to 35% (wet basis).

Table 1 showed that the samples considered in this study matched with the requirements. The ash content, sulfur and chlorine contents met the requirements. Mercury content, not shown in Table 1, was below the quantification limit of 0.1 mg/kg_{DM} and also met the requirements. The LHV, between 18 and 21 MJ/kg, was in the high range of the requirements. The ash melting point was not

measured in this study. It is known to increase with Si, Ti and Al contents and to decrease when the contents in Fe, Ca, Mg, K and Na increase [30].
Finally, VM contents were also in the favorable range for 3P-I-T and 3P-A-F samples or slightly below for 2P-I-S sample with 73.5% (Table 1).

As for biochemical composition, several authors reported that thermochemical decomposition of biomass with a higher content in cellulose and hemicelluloses was faster and produced a larger fraction of gaseous products than that of biomass with a higher lignin content, which leads to a larger fraction of solid products [51;52]. Moreover, cellulose and hemicelluloses were reported to produce more CO and CH_4 and less H_2 and CO_2 than lignin, i.e. biomass with more lignin produces more hydrogen than others [53].
According to Collard and Blin [44], the high content of benzene rings in lignin explains the high char yield. Therefore, the use of biomass with high lignin content is recommended for the production of char for energy or other industrial or agronomic applications. The samples studied here were found to have a moderate lignin content of 13−16% w/w (Table 1) as compared to other lignocellulosic biomasses [25].

As indicated above, olive mill solid residues must be agglomerated by pelletization or briquetting before fueling a gasifier in order to increase their bulk density. The residual oil content may however reduce the quality of the pellet and the densification process [54]. According to Kalyan and Morey [55], oil content should not exceed 6.5% to allow the effective formation of pellets. The typical content in residual olive oil in olive mill solid residues is considered to range between 5 and 8% depending on the extraction technology [56]. Yaman et al. [57] reported that the addition of olive residues had detrimental effects on the mechanical strength of biomass briquettes. Possible solutions to match the requirements are blending the olive pomace with other oil-free biomasses, or to extract residual oil with a volatile solvent such as hexane which can be easily recovered by distillation.

4.2 Post-treatment of syngas and energy recovery
The downstream technology selected for syngas treatment may have an incidence on the type and nature of biomass to feed the gasifier. Gas specifications are different for the various gas applications and the composition of syngas is very dependent on the type of gasification process, gasification agent and other parameters such as temperature.
Based on the general composition and the typical applications, two main types of gasification gas can be distinguished, i.e. "biosyngas", produced by high temperature gasification (above 1200 °C) or catalytic gasification, and "product gas", produced by low temperature gasification (below 1000 °C) [58].
The major application of product gas will be the direct use for the generation of power (and heat). This can be either in stand-alone combined heat and power (CHP) plants or by co-firing of the product gas in large-scale power plants. The second major application of product gas is the production of synthetic natural gas (SNG). SNG is a gas with similar properties as natural gas but produced by methanation (either catalytic methanation or biomethanation, i.e. involving the action of micro-organisms) [58;59].
Utilization of biosyngas include power generation, transportation fuels (Fischer-Tropsch synthesis, production of methanol), chemical synthesis (ammonia for fertilizer production, hydroformylation of olefins (i.e. production of aldehydes), production of hydrogen to be used in refineries, SNG production) [58].

A promising alternative for the production of biofuels and valuable chemicals from syngas is microbial syngas fermentation. This technology has significant advantages over the metal catalytic pathway (Fischer-Tropsch synthesis for instance) [60;61].
Both gases need additional gas cleaning and conditioning to afford a gas with the correct composition and specifications for the final application.

4.3 Resource availability and potential energy production

Relevant updated data and information regarding the production and availability of olive mill solid residues over the world are relatively scarce. In a report published in 2008 [62], the estimated amount of residues was about 1.5 million tons, including stones and exhausted olive pomace. In a more recent study, the world olive oil production was estimated at 2.95 million tons [63]. Most olive oil (98%) was produced in the Mediterranean region. About 73% of the production was coming from the European Union (EU), mostly Spain, Italy and Greece which accounted for about 97% of EU olive oil production [63;64]. Considering an average production of 0.63 kg DM of solid residues per kg of olive oil (ca. 0.51 kg for a two-phase extraction process and ca. 0.75 kg for a three-phase one) [1], a production of around 1.8 million tons of solid residues can be estimated.
A preliminary pilot-scale gasification test was performed using a downdraft co-current fixed-bed gasifier (unpublished results). The reactor was operated with a feed of 12.5 kg/h of 2P-I-S olive mill residue dried to a moisture content around 12% (i.e 11.0 kg/h of dry biomass). Since the LHV of the 2P-I-S sample was 18.3 MJ/kg_{DM}, the feed of 11.0 kg DM/h corresponded to an input of ca. 200 MJ/h or 55.9 kW. The pilot delivered 43.8 kW in the form of syngas, corresponding to an energy yield of 43.8/55.9 = 0.78.
Based on these orders of magnitude, the overall production of 1.8 million tons of olive mill solid residues estimated above would represent, in a simplified preliminary approach, an overall annual energy potential of $1.8\ 10^6 \times 18.3$ GJ, i.e. ca. $32.9\ 10^6$ GJ or ca. 9,150 GWh. This annual potential resources would be equivalent to around $7.87\ 10^5$ of TOE (tons of oil equivalent).

5. Conclusions

The results obtained from the analyses of three olive mill solid residues of different origins underlined their complex nature and composition and the influence of several factors such as the type of process used for olive oil extraction, the local conditions of operation, but also probably the olive fruit varieties, cultivation conditions, and climate. Total mass losses in the range of 91-95% w/w of dry matter were recorded from TG analyses in air, indicating that the residues were mainly organic, with relatively low inorganic content, although higher than classically observed in wood. The high organic content was a favorable parameter in the perspective of using these residues as fuels for gasification. Overall mass losses measured in N_2 were lower than in air however, in the range of 80-84% w/w of dry matter. TG-DSC analyses along with fiber analyses showed the presence of several types of organic constituents, including cellulose, hemicelluloses and lignin.
TG-DSC and FTIR revealed some differences of composition, which were mainly attributed to the influence of the process used for olive oil extraction.
Py-GC/MS results allowed to identify the nature of some of the organic constituents in the pyrolysis gas, such as phenolic compounds formed by lignin pyrolysis, or oleic acid and derivatives produced by vaporization or pyrolysis of residual olive oil.

The sample originating from a two-phase extraction process followed by hexane extraction of residual oil exhibited the highest analytical differences with the other two samples, thereby revealing the effect of the olive oil extraction process on the composition of the residues.
Finally, the composition of the residues met the requirements for gasification for most parameters.

Acknowledgements
This study was part of an ERA-NET MED research program (BIOSOL) aiming at the development and demonstration of a hybrid renewable electricity production mini-power plant, composed of a concentrated solar power system and a biomass gasification boiler operated with solid residues from olive oil production. The authors wish to thank the French Agence Nationale de la Recherche (ANR) for financial support.
The authors also wish to thank ENIT for sending the 3P-I-T sample and Nathalie Dumont for fiber analysis.

References
[1] A.G. Vlyssides, M. Loizides, P.K. Karlis, Integrated strategic approach for reusing olive oil extraction by-products, J. Clean. Prod. 12 (2004) 603−611. doi:10.1016/S0959-6526(03)00078-7.
[2] A. Roig, M.L. Cayuela, M.A. Sánchez-Monedero, An overview on olive mill wastes and their valorisation methods, Waste Manage. 26 (2006) 960−969. doi:10.1016/j.wasman.2005.07.024.
[3] E. Christoforou, P.A. Fokaides, A review of olive mill solid wastes to energy utilization techniques, Waste Manage. 49 (2016) 346–363. doi:10.1016/j.wasman.2016.01.012.
[4] F. Pagnanelli, C.C. Viggi, L. Toro, Development of new composite biosorbents from olive pomace wastes, Appl. Surf. Sci., 256 (2010) 5492−5497. doi:10.1016/j.apsusc.2009.12.146.
[5] A.C. Caputo, F. Scacchia, P.M. Pelagagge, Disposal of by-products in olive oil industry: waste-to-energy solutions, Appl. Therm. Eng. 23 (2003) 197−214. https://doi.org/10.1016/S1359-4311(02)00173-4.
[6] A.R. Tekin, A.C. Dalgıç, Biogas production from olive pomace, Resour. Conserv. Recycl. 30 (2000) 301−313.
[7] R. Borja, B. Rincón, F. Raposo, J. Alba, A. Martín, A study of anaerobic digestibility of two-phases olive mill solid waste (OMSW) at mesophilic temperature, Process Biochem. 38 (2002) 733−742.
[8] B. Fezzani, R. Ben Cheikh, Thermophilic anaerobic co-digestion of olive mill wastewater with olive mill solid wastes in a tubular digester, Chem. Eng. J. 132 (2007) 195−203. doi:10.1016/j.cej.2006.12.017.
[9] E.C. Koutrouli, H. Kalfas, H.N. Gavala, I.V. Skiadas, K. Stamatelatou, G. Lyberatos, Hydrogen and methane production through two-stage mesophilic anaerobic digestion of olive pulp, Bioresour. Technol. 100 (2009) 3718−3723. doi:10.1016/j.biortech.2009.01.037.
[10] B. Rincón, R. Borja, M.A. Martín, A. Martín, Kinetic study of the methanogenic step of a two-stage anaerobic digestion process treating olive mill solid residue, Chem. Eng. J. 160 (2010) 215−219. doi:10.1016/j.cej.2010.03.046.
[11] V. Riggio, E. Comino, M. Rosso, Energy production from anaerobic codigestion processing of cow slurry, olive pomace and apple pulp, Renew. Energy 83 (2015) 1043–1049. http://dx.doi.org/10.1016/j.renene.2015.05.056
[12] A. Siciliano, M.A. Stillitano, S. De Rosa, Biogas production from wet olive mill wastes pretreated with hydrogen peroxide in alkaline conditions, Renew. Energy 85 (2016) 903−916. http://dx.doi.org/10.1016/j.renene.2015.07.029.
[13] A. Zabaniotou, G. Kalogiannis, E. Kappas, A. Karabelas, Olive residues (cuttings and kernels) rapid pyrolysis product yields and kinetics, Biomass Bioenergy 18 (2000) 411−420.
[14] M.C. Blanco Lopez, C.G. Blanco, A. Martinez-Alanso, Composition of gases release during olive stones pyrolysis, J. Anal. Appl. Pyrolysis 65 (2002) 313−322.

[15] F. Jurado, A. Cano, J. Carpio, Modelling of combined cycle power plants using biomass, Renew. Energy 28 (2003) 743−753.
[16] P. García-Ibañez, A. Cabanillas, J.M. Sánchez, Gasification of leached orujillo (olive oil waste) in a pilot plant circulating fluidised bed reactor. Preliminary results, Biomass Bioenergy 27 (2004) 183−194. doi:10.1016/j.biombioe.2003.11.007.
[17] A.E. Pütün, B.B. Uzun, E. Apaydın, E. Pütün, Bio-oil from olive oil industry wastes: pyrolysis of olive residue under different conditions, Fuel Process. Technol. 87 (2005) 25−32. doi:10.1016/j.fuproc.2005.04.003.
[18] R.N. André, F. Pinto, C. Franco, M. Dias, I. Gulyurtlu, M.A.A. Matos, I. Cabrita, Fluidised bed co-gasification of coal and olive oil industry wastes, Fuel 84 (2005) 1635−1644. doi:10.1016/j.fuel.2005.02.018.
[19] J.F. González, S. Román, D. Bragado, M. Calderón, Investigation on the reactions influencing biomass air and air/steam gasification for hydrogen production, Fuel Process. Technol. 89 (2008) 764−772. doi:10.1016/j.fuproc.2008.01.011.
[20] V. Skoulou, G. Koufodimos, Z. Samaras, A. Zabaniotiou, Low temperature gasification of olive kernels in a 5-kW fluidized bed reactor for H_2-rich producer gas, Int. J. Hydrogen Energy 33 (2008) 6515−6524. doi:10.1016/j.ijhydene.2008.07.074.
[21] V. Skoulou, A. Swiderski, W. Yamg, A. Zabaniotou, Process characteristics and products of olive kernel high temperature steam gasification (HTSG), Bioresour. Technol. 100 (2009) 2444−2451. doi:10.1016/j.biortech.2008.11.021
[22] C. Guizani, K. Haddad, M. Jeguirim, B. Colin, L. Limousy, Combustion characteristics and kinetics of torrefied olive pomace. Energy 107 (2016) 453−463. http://dx.doi.org/10.1016/j.energy.2016.04.034.
[23] I. Ghouma, M. Jeguirim, C. Guizani, A. Ouederni, L. Limousy, Pyrolysis of Olive Pomace: Degradation Kinetics, Gaseous Analysis and Char Characterization, Waste Biomass Valor. 8 (2017) 1689−1697. doi:10.1007/s12649-017-9919-8.
[24] A. Gomez-Martin, R. Chacartegui, J. Ramirez-Rico, J. Martinez-Fernandez, Performance improvement in olive stone's combustion from a previous carbonization transformation, Fuel 228 (2018) 254–262. doi:10.1016/j.fuel.2018.04.127.
[25] V. Dhyani, T. Bhaskar, A comprehensive review on the pyrolysis of lignocellulosic biomass, Renew. Energy 129 (2018) 695−716. http://dx.doi.org/10.1016/j.renene.2017.04.035.
[26] Norme XP U44-162, Amendements organiques et supports de culture - Fractionnement biochimique et estimation de la stabilité biologique - Méthode de caractérisation de la matière organique par solubilisations successives (2005).
[27] P.J. Van Soest, R.H. Wine, Use of detergents in the analysis of fibrous feeds. IV. Determination of plant cell-wall constituents, J. Assoc. Offic. Anal. Chem. 50 (1967) 50−55.
[28] S. Arvelakis, H. Gehrmann, M. Beckmann, E.G. Koukios, Agglomeration problems during fluidized bed gasification of olive-oil residue: evaluation of fractionation and leaching as pre-treatments, Fuel 82 (2003) 1261−1270. doi:10.1016/S0016-2361(03)00013-9.
[29] J. Giuntoli, S. Arvelakis, H. Spliethoff, W. de Jong, A.H.M. Verkooijen, Quantitative and kinetic Thermogravimetric Fourier Transform Infrared (TG-FTIR) study of pyrolysis of agricultural residues: influence of different pretreatments, Energy Fuels 23 (2009) 5695−5706. doi:10.1021/ef9005719.
[30] L.I. Darvell, J.M. Jones, B. Gudka, X.C. Baxter, A. Saddawi, A. Williams, A. Malmgren, Combustion properties of some power station biomass fuels, Fuel 89 (2010) 2881−2890. doi:10.1016/j.fuel.2010.03.003.
[31] C.N.R. Rao, Chemical Applications of Infrared Spectroscopy, Academic, London, UK, 1963.
[32] N. Tena, R. Aparicio, D.L. García-González, Virgin olive oil stability study by mesh cell-FTIR spectroscopy, Talanta 167 (2017) 453−461. https://doi.org/10.1016/j.talanta.2017.02.042.
[33] O. Francioso, S. Sánchez-Cortés, D. Casarini, J.V. Garcia-Ramos, C. Ciavatta, C. Gessa, Spectroscopic study of humic acids fractionated by means of tangential ultrafiltration, J. Mol. Struct. 609 (2002) 137–147. doi:10.1016/s0022-2860(01)00971-1.
[34] O. Francioso, E. Ferrari, M. Saladini, D. Montecchio, P. Gioacchini, C. Ciavatta, TG–DTA, DRIFT

and NMR characterisation of humic-like fractions from olive wastes and amended soil, J. Hazard. Mater. 149 (2007) 408–417. doi:10.1016/j.jhazmat.2007.04.002.
[35] U. Tomati, E. Madejon, E. Galli, D. Capitani, A.L. Segre, Structural changes of humic acids during olive mill pomace composting, Compost Sci. Util. 9 (2001) 134–142. doi:10.1080/1065657x.2001.10702027.
[36] H. Yang, J. Irudayaraj, Comparison of near-infrared, Fourier transform-infrared, and Fourier transform-Raman methods for determining olive pomace oil adulteration in extra virgin olive oil, J. Am. Oil Chem. Soc. 78 (2001) 889–895.
[37] M. Amutio, G. Lopez, R. Aguado, M. Artetxe, J. Bilbao, M. Olazar, Kinetic study of lignocellulosic biomass oxidative pyrolysis, Fuel 95 (2012) 305−311. doi:10.1016/j.fuel.2011.10.008.
[38] S. Vecchio, L. Cerretani, A. Bendini, E. Chiavaro, Thermal decomposition study of monovarietal extra virgin olive oil by simultaneous thermogravimetry/differential scanning calorimetry: relation with chemical composition, J. Agric. Food Chem. 57 (2009) 4793–4800. doi:10.1021/jf900120v.
[39] H. Yang, R. Yan, H. Chen, C. Zheng, D.H. Lee, D.T. Liang, In-depth investigation of biomass pyrolysis based on three major components: hemicellulose, cellulose and lignin, Energy Fuels 20 (2006) 388–393. doi: 10.1021/ef0580117.
[40] M. Brebu, C. Vasile, Thermal degradation of lignin – a review, Cellul. Chem. Technol. 44 (2010) 353–363.
[41] G.C. Galletti, P. Bocchini, Pyrolysis/gas chromatography/mass spectrometry of lignocellulose, Rapid Commun. Mass Spectrom. 9 (1995) 815–826.
[42] R. Fahmi, A.V. Bridgwater, S.C. Thain, I.S. Donnison, P.M. Morris, N. Yates, Prediction of Klason lignin and lignin thermal degradation products by Py–GC/MS in a collection of Lolium and Festuca grasses, J. Anal. Appl. Pyrolysis 80 (2007) 16–23. doi:10.1016/j.jaap.2006.12.018.
[43] Q. Lu, X.C. Yang, C.Q. Dong, Z.F. Zhang, X.M. Zhang, X.F. Zhu, Influence of pyrolysis temperature and time on the cellulose fast pyrolysis products: Analytical Py-GC/MS study, J. Anal. Appl. Pyrolysis 92 (2011) 430–438. doi:10.1016/j.jaap.2011.08.006.
[44] F.X. Collard, J. Blin, A review on pyrolysis of biomass constituents: Mechanisms and composition of the products obtained from the conversion of cellulose, hemicelluloses and lignin, Renew. Sustain. Energy Rev. 38 (2014) 594–608. http://dx.doi.org/10.1016/j.rser.2014.06.013.
[45] I. Schmeltz, W.S. Schlotzhauer, E.B. Higman, Characteristic products from pyrolysis of nitrogenous organic substances. Beitr. Tabakforsch./Contrib. Tob. Res. 6 (1972) 134–138. DOI:10.2478/cttr-2013-0281.
[46] T. Gutfinger, Polyphenols in olive oils, J. Am. Oil Chem. Soc. 58 (1981) 966–968.
[47] G. Papadopoulos, D. Boskou, Antioxidant effect of natural phenols on olive oil, J. Am. Oil Chem. Soc. 68 (1991) 669–671.
[48] H.L. Newmark, Squalene, olive oil, and cancer risk: a review and hypothesis, Cancer Epidemiol. Prev. Biomark. 6 (1997) 1101–1103.
[49] D. Stapf, G. Ceceri, I. Johansson, K. Whitty, Biomass pre-treatment for bioenergy. Case study 3: Pretreatment of municipal solid waste (MSW) for gasification, IEA Bioenergy, 2019.
[50] M.I. Al-Widyan, H.F. Al-Jalil, Stress-density relationship and energy requirement of compressed olive cake, Appl. Eng. in Agricult. 17 (2001) 749–753.
[51] A. Gani, I. Naruse, Effect of cellulose and lignin content on pyrolysis and combustion characteristics for several types of biomass, Renew. Energy 32 (2007) 649–661. doi:10.1016/j.renene.2006.02.017.
[52] L. Burhenne, J. Messmer, T. Aicher, M.P. Laborie, The effect of the biomass components lignin, cellulose and hemicellulose on TGA and fixed bed pyrolysis, J. Anal. Appl. Pyrolysis 101 (2013) 177–184. http://dx.doi.org/10.1016/j.jaap.2013.01.012.
[53] T. Tian, Q. Li, R. He, Z. Tan, Y. Zhang, Effects of biochemical composition on hydrogen production by biomass gasification, Int. J. Hydrogen Energy 42 (2017) 19723–19732. http://dx.doi.org/10.1016/j.ijhydene.2017.06.174.
[54] M. Barbanera, E. Lascaro, V. Stanzione, A. Esposito, R. Altieri, M. Bufacchi, Characterization of pellets from mixing olive pomace and olive tree pruning, Renew. Energy 88 (2016) 185–191.

http://dx.doi.org/10.1016/j.renene.2015.11.037.
[55] N. Kaliyan, R.V. Morey, Factors affecting strength and durability of densified biomass products, Biomass Bioenergy 33 (2009) 337–359. doi:10.1016/j.biombioe.2008.08.005.
[56] I. Doymaz, O. Gorel, N.A. Akgun, Drying characteristics of the solid by-product of olive oil extraction, Biosyst. Eng. 88 (2004) 213–219. doi:10.1016/j.biosystemseng.2004.03.003.
[57] S. Yaman, M. Sahan, H. Haykiri-Acma, K. Sesen, S. Kücükbayrak, Fuel briquettes from biomass-lignite blends, Fuel Processing Technology 72 (2001) 1–8.
[58] H. Boerrigter, R. Rauch, Review of applications of gases from biomass gasification, Report from Energy research Centre of the Netherlands (ECN), ECN Biomass, Coal & Environmental research, ECN-RX--06-066, 2006.
[59] A. Grimalt-Alemany, I.V. Skiadas, H.N. Gavala, Syngas biomethanation: state-of-the-art review and perspectives, Biofuels, Bioprod. Bioref. 12 (2018) 139–158. DOI: 10.1002/bbb.1826.
[60] P.C. Munasinghe, S.K. Khanal, Biomass-derived syngas fermentation into biofuels: opportunities and challenges, Bioresour. Technol. 101 (2010) 5013–5022. doi:10.1016/j.biortech.2009.12.098.
[61] M. El-Gammal, R. Abou-Shanab, I. Angelidaki, B. Omar, P.V. Sveding, D.B. Karakashev, Y. Zhang, High efficient ethanol and VFA production from gas fermentation: Effect of acetate, gas and inoculum microbial composition, Biomass Bioenergy 105 (2017) 32–40. http://dx.doi.org/10.1016/j.biombioe.2017.06.020.
[62] MORE, Market of Olive Residues for Energy, Intelligent Energy for Europe (IEE) project, Deliverable 3.1, One joint report for the 5 Regional "state of the art" reports from each involved area describing the current olive-milling residues market with a focus on energy uses, 2008.
[63] M.K. Doula, J.L. Moreno-Ortego, F. Tinivella, V.J. Inglezakis, A. Sarris, K. Komnitsas, Olive mill waste: recent advances for the sustainable development of olive oil industry, in: C.M. Galanakis (Ed.), Olive Mill Waste, Academic Press, 2017, pp. 29–56.
[64] European Commission, Directorate-General for Agriculture and Rural Development, Economic analysis of the olive sector, Latest update: July 2012.